Ultrasound in Med. & Biol., Vol. 33, No. 8, pp. 1285–1295, 2007

0301-5629/07/$–see front matter

ELSEVIER

doi:10.1016/j.ultrasmedbio.2007.02.005

● *Original Contribution*

ULTRASOUND-INDUCED THERMAL ELEVATION IN CLOTTED BLOOD AND CRANIAL BONE

VOLODYMYR NAHIRNYAK, T. DOUGLAS MAST, and CHRISTY K. HOLLAND
Department of Biomedical Engineering, University of Cincinnati, Cincinnati, OH, USA

(*Received* 15 *August* 2006, *revised* 6 *January* 2007, *in final form* 9 *February* 2007)

Abstract—Ultrasound thermal effects have been hypothesized to contribute to ultrasound-assisted thrombolysis. To explore the thermal mechanism of ultrasound-enhanced thrombolysis with recombinant tissue plasminogen activator (rt-PA) for the treatment of ischemic stroke, a detailed investigation is needed of the heating produced in skull, brain and blood clots. A theoretical model is developed to provide an estimate for the worst-case scenario of the temperature increase in blood clots and on the surface of cranial bone exposed to 0.12- to 3.5-MHz ultrasound. Thermal elevation was also assessed experimentally in human temporal bone, human clots and porcine clots exposed to 0.12 to 3.5-MHz pulsed ultrasound *in vitro* with a peak-to-peak pressure of 0.25 MPa and 80% duty cycle. Blood clots exposed to 0.12-MHz pulsed ultrasound exhibited a small temperature increase (0.25° C) and bone exposed to 1.0-MHz pulsed ultrasound exhibited the highest temperature increase (1.0° C). These experimental results were compared with the predicted temperature elevations. (E-mail: nahirnvm@email.uc.edu) **© 2007 World Federation for Ultrasound in Medicine & Biology.**

Key Words: **Ultrasound, Hyperthermia, Thrombolysis.**

INTRODUCTION

Recent studies of ultrasound-enhanced thrombolysis have indicated the possibility of using lower exposure levels (<2.5 W/cm^2) in combination with thrombolytic drugs for restoration of blood flow in the arteries in the heart, legs and brain (Rosenschein et al. 1997; Atar 2001; Atar et al. 2001; Atar and Rosenschein 2004; Pfaffenberger et al. 2005; Alexandrov et al. 2004). Also, lower-intensity therapeutic ultrasound applications are under investigation to promote gene transfection and enhanced drug delivery (Bekeredjian et al. 2003; Taniyama et al. 2002).

Recombinant tissue plasminogen activator (rt-PA) is moderately effective in lysing thrombi in ischemic stroke patients and improves neurologic deficits if given within three hours after the onset of stroke symptoms (Wolpert et al. 1993). Unfortunately, thrombolytics also can cause intracerebral hemorrhage. Thus an adjuvant therapy that lowers the systemic dose of rt-PA or increases its thrombolytic efficacy would represent a significant breakthrough.

Address correspondence to: Volodymyr Nahirnyak, Department of BME, University of Cincinnati, Medical Science Building, Rm. 6155, 231 Albert Sabin Way, Cincinnati, OH 45267-0586. E-mail: nahirnvm@email.uc.edu

Effective methods of enhancing thrombolysis have been examined in an attempt to reduce the dosage of the thrombolytic agent and reduce the risk of hemorrhagic events. Kudo (1989) extended the use of therapeutic ultrasound to increase the efficacy of systemic rt-PA. They delivered transcutaneous 200-kHz continuous wave ultrasound to enhance rt-PA–induced fibrinolysis in a canine femoral arterial thrombus model. Lauer et al. (1992) demonstrated that 1-MHz intermittent ultrasound, with an exposure interval of 2 s followed by a quiescent interval of 2 s, increased the percent mass loss in a whole human blood clot model *in vitro*. They proposed that acoustic streaming alone, without cavitational effects, was responsible for the increased thrombolysis. Careful investigations by Francis and his coworkers suggest that ultrasound accelerates enzymatic fibrinolysis by increasing transport of reactants through a cavitation-related mechanism (Francis et al. 1992; Blinc et al. 1993; Francis et al. 1995). However, experiments using ultrasound exposure of clots in a hyperbaric chamber revealed that other mechanisms in addition to inertial cavitation were present (Everbach and Francis 2000).

Several investigators have utilized transcranial, low-frequency, low-intensity ultrasound to accelerate thrombolysis (Akiyama et al. 1998; Behrens et al. 1999; Shaw et al. 2001a, 2001b) and Holland et al. (2002)

provided experimental evidence *in vitro* that ultrasound can be used in combination with rt-PA to increase thrombus dissolution in porcine and human clot models. Suchkova et al. (2002) explored ultrasound-enhanced fibrinolysis at low kilohertz frequencies (27–100 kHz) in an attempt to minimize ultrasonic heating and concomitant adverse bioeffects (McDannold et al. 2004; Duckett et al. 2004; Vella et al. 2003). In addition, clinical trials conducted by Alexandrov et al. (2004) have shown efficacy of ultrasound-enhanced thrombolysis in the treatment of ischemic stroke in patients.

Mild heating of only a few degrees can increase the enzymatic activity of rt-PA and can contribute to the enhanced thrombolysis (Shaw et al. 2006). The rates of particle diffusion and biochemical reactions are both temperature dependent (Cheng 1981). Also, an increase in temperature can affect membrane permeability, active transport processes and metabolic rates (Nyborg and Ziskin 1985). Enzymatic biochemical reaction rates increase with rising temperature to a specific temperature threshold, where the enzyme becomes denatured and the reaction rate subsequently declines (Cheng 1981). Thus one would expect that a thermal mechanism could contribute to enhanced thrombolysis in the presence of ultrasound hyperthermia.

Sakharov et al. (2000) and Shaw et al. (2003) have explored the contribution of enhanced thrombolysis as a result of mild hyperthermia in the absence of ultrasound exposure. The effects of a 6° C temperature rise above 37° C on the lytic rate in a human plasma clot model were measured *in vitro* by Sakharov et al. (2000). A 6° C temperature increase caused a doubling in the percent lysis after a 30-min exposure to this elevated temperature. Similarly, Sakharov et al. (2000) explored the contribution of stirring on the observed enhanced thrombolysis. Sakharov et al. (2000) hypothesized that the acceleration of enzymatic plasma clot lysis as a result of ultrasound exposure was caused by the effects of both heating and acoustic streaming. However, neither of these ultrasonic effects was observed or measured directly. Because the thermal effects do not account solely for the observed enhancement of thrombolysis, many authors have concluded that this enhancement is the result of a combination of mechanical and thermal mechanisms (Dick et al. 1998; Francis et al. 1992; Lauer et al. 1992; Blinc et al. 1993; Harpaz et al. 1993; Olsson et al. 1994; Sakharov et al. 2000).

In this study, we explore the extent of heating with ultrasound parameters in the range used for ultrasound-enhanced thrombolysis studies (Holland et al. 2002; Shaw et al. 2001a, 2001b; Alexandrov et al. 2004) by deriving an analytic model of hyperthermia in clotted blood exposed to 0.12-MHz, 1.0-MHz and 3.5-MHz pulsed ultrasound. For such a model to be developed, the acousto-mechanical and thermal properties of clotted blood must be well characterized. We rely on the previous study of the acousto-mechanical and thermal properties of clotted blood as inputs for this model (Nahirnyak et al. 2005, 2006).

The investigation of the transcranial transmission losses through a human skull demonstrated mild attenuation (22.5%) of the ultrasound beam at 120 kHz (Coussios et al. 2002). A larger amount of heating at the surface of the cranial bone would be expected at higher frequencies. To investigate this concern, we performed numerical estimates for the temperature rise on the front face of human skull using the results of the theory developed by Nyborg (1988).

The thermal elevation was also assessed experimentally in clotted blood and human temporal bone exposed to pulsed ultrasound *in vitro* with the same range of center frequencies (0.12 MHz, 1.0 MHz and 3.5 MHz). These experimental results were compared with the predicted temperature elevation in clotted blood and bone.

METHODS

Theoretical model

Absorption of ultrasound can cause a temperature increase in soft tissue and bone. By knowing the intensity of ultrasound in the tissue and the physical properties of the surrounding material, it is possible to calculate theoretically the expected thermal elevation in both soft tissue and cranial bone for the *in-vitro* case investigated in this work. For this purpose we need, namely, the coefficient of acoustic absorption, density, specific heat and thermal conductivity of clotted blood and cranial bone.

To determine the spatial and temporal dependence of temperature elevation $T(\vec{R}, t)$ in our experimental blood clots exposed to pulsed ultrasound, we chose to solve the bio-heat transfer equation for an idealized spherical tissue insonified by plane waves (see Figs. 1 and 2). The bio-heat transfer equation in the tissue characterized by thermal conductivity K, density ρ and specific heat, C_m, ignoring perfusion, is given by the following equation (Nyborg 1988):

$$\nabla_r^2 T - \frac{1}{\kappa}\frac{\partial T}{\partial t} = -\frac{2\alpha I}{K} = -4\pi\,\Psi(\vec{r}, t), \qquad (1)$$

where $\kappa = \dfrac{K}{\rho C_m}$ is the thermal diffusivity of tissue, α is the amplitude absorption coefficient in the blood clot, I is the spatial average, temporal average intensity in the incident ultrasonic wave, $\Psi(\vec{r}, t)$ is the heat source function, $\vec{r}$ is the radius vector from the center of the clot and t is time. Only a radial term appears in the expression for the Laplacian operator, because in our model we consider the clot as an absorbing sphere of radius a, where

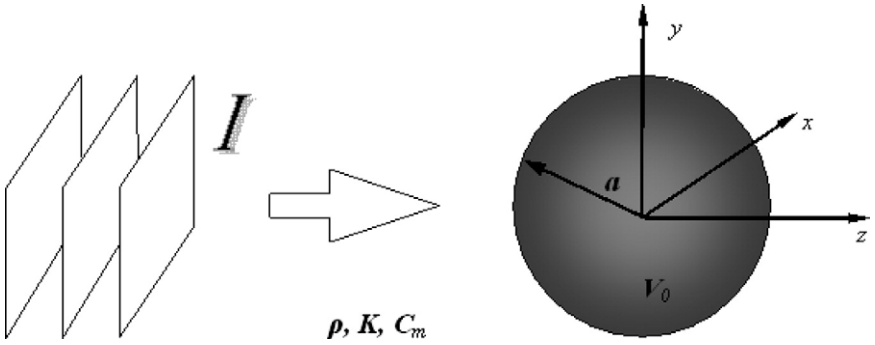

Fig. 1. The geometry used to model the hyperthermia of a spherical blood clot of radius, a, surrounded by fluid and insonified with ultrasound. Density, ρ, specific heat C_m and thermal conductivity K were assumed to be identical for the clot and surrounding fluid. The intensity of the incident infinite plane acoustic wave is I.

the absorption of acoustic energy occurs only within the limits of the blood clot:

$$\Psi(\vec{r}, t) = \frac{\alpha I}{2\pi K} \quad \text{for } r \le a, \text{ and}$$

$$\Psi(\vec{r}, t) = 0 \quad \text{for } r > a. \tag{2}$$

The amplitude absorption coefficient, α, is defined by the following expression for the spatial dependence of the time-averaged intensity of an acoustic wave in a medium with no scattering (NCRP 1992):

$$I(z) = I_0 e^{-2\alpha z} \quad \text{for } z \ge 0, \tag{3}$$

where I_0 is the initial ultrasound intensity.

Because of heat conduction from the heat source, there is heat flux away from the clot or bone into the surrounding medium (assumed to be water). In our model, we disregard heat convection as a result of perfusion, which may contribute to the loss of heat generated inside the insonified tissue. The solution to eqn (1), with homogeneous boundary conditions, $T(0, 0) = 0$ and $T(\infty, t) = 0$, is given by the following integral equation (Morse and Feshbach 1953):

$$T(\vec{R}, t) = \int_0^t \int_{V_0} \Psi(\vec{r}, \tau) G(\vec{R}, t \mid \vec{r}, \tau)\, dV_0\, d\tau, \tag{4}$$

where the volume, V_0, within the clot boundaries is shown in Fig. 1 and τ is the temporal integration variable. The Green's function for eqn (1) is:

$$G(\vec{R}, t \mid \vec{r}, \tau) = \frac{\exp\left\{-\dfrac{\left|\vec{R}-\vec{r}\right|^2}{4\kappa\tau}\right\}}{2\pi^{1/2}\kappa^{1/2}\tau^{3/2}}\, u(t). \tag{5}$$

where $u(t)$ is a step function.

For the spatial and temporal dependence of the temperature rise we have:

$$T(\vec{R}, t) = \frac{\alpha I}{4\pi^{3/2}\kappa^{1/2} K} \int_0^t \frac{1}{\tau^{3/2}} \int_0^{2\pi} \int_0^{\pi} \int_0^{a} \exp\left\{-\frac{R^2 + r^2 - 2Rr\cos\theta}{4\tau\kappa}\right\} r^2 \sin\theta\, dr\, d\theta\, d\varphi\, d\tau,$$

$$\text{for } t \ge 0, \tag{6}$$

where θ and φ are the spherical angular coordinates. Be-

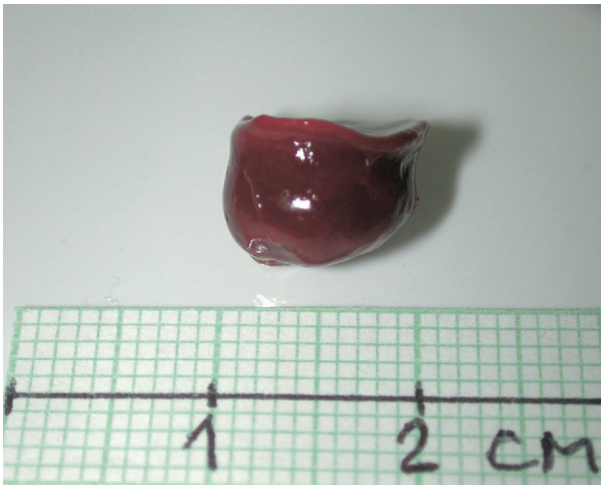

Fig. 2. Photograph of a blood clot sample. Whole blood clots were prepared from either fresh porcine or human blood by aliquoting 1.5 or 2.0 mL into 10-mL glass tubes (Vacutainer), immersing the tubes in a 37° C water bath for three hours and storing the clots at 5° C for at least three days before assessment of the properties, which ensured complete clot retraction. The typical size of the clot samples was about 7 to 10 mm in diameter with a mass of about 0.5 g.

cause the error function is odd, *i.e.*, $\mathrm{erf}(-\eta) = -\mathrm{erf}(\eta)$, we may write the final expression for the temperature rise in the following form:

$$T(\vec{R}, t) = \frac{2\alpha I\kappa^{3/2}}{\pi^{1/2}K}\frac{1}{R}\int_0^t \left(\exp\left\{-\frac{(a+R)^2}{4\tau\kappa}\right\} - \exp\left\{-\frac{(a-R)^2}{4\tau\kappa}\right\}\right)\tau^{1/2}\,d\tau + \frac{\alpha I\kappa}{K}\int_0^t \left[\mathrm{erf}\left\{\frac{a-R}{2\sqrt{\tau\kappa}}\right\} + \mathrm{erf}\left\{\frac{a+R}{2\sqrt{\tau\kappa}}\right\}\right]d\tau. \quad (7)$$

At the center of a clot ($R = 0$), we have:

$$T(0,\ t) = \frac{2\alpha I\kappa}{K}\int_0^t \mathrm{erf}\left\{\frac{a}{2\sqrt{\tau\kappa}}\right\}d\tau + \frac{2\alpha Ia}{K}\sqrt{\frac{\kappa}{\pi}}\int_0^t \frac{\exp\left\{-\frac{a^2}{4\tau\kappa}\right\}}{\sqrt{\tau}}\,d\tau = \frac{\alpha Ia^2}{K}\left[1 - \frac{1}{\sqrt{\pi}}\sqrt{\frac{t}{\tau_h}}\exp\left(-\frac{\tau_h}{t}\right) - \left(1 - \frac{t}{2\tau_h}\right)\mathrm{erf}\left(\sqrt{\frac{\tau_h}{t}}\right)\right], \quad (8)$$

where $\tau_h = \dfrac{a^2}{4\kappa}$ is the time constant for heating.

For small values of the time, eqn (8) reduces to the following expression for the temperature rise inside the clot:

$$T(\vec{R}, t) = \frac{2\alpha\, I}{\rho C_m}t, \quad (9)$$

which corresponds to simple adiabatic heating of a clot by ultrasound (Nyborg 1978).

Equation (8) gives the values for the steady state temperature increase at the center of the blood clot after a long period of insonification ($t = \infty$):

$$T(0, \infty) = \frac{\alpha Ia^2}{K}. \quad (10)$$

The temperature elevation at the center of a bone disk, $T_{bone}(0,0,t)$, insonified with a spatial peak temporal average intensity, I_{SPTA}, can be calculated by the following formula (Nyborg 1988; Nyborg and Wu 1994):

$$T_{bone}(0, 0, t) = \frac{1}{8\pi K_{sk}}\int_0^\infty q_v(r, z)F(r, t\,)\,dV, \quad (11)$$

where $q_v(r,z)$ is the volume rate of heat generation from the absorption in skull bone characterized by the coefficient of thermal conductivity, K_{sk}, V is the cylindrical volume of the skull disk exposed to ultrasound and $F(r,\ t)$ is a function proportional to the temperature rise from a small volumetric heat source. Because perfusion is neglected in our model, the function $F(r, t)$ reduces to 2 for large values of time (Carstensen et al. 1990). We also assume that the heating of the skull bone occurs within the limits of –3 dB beam width (BW). Then, the steady state temperature elevation is given by the integral:

$$T_{bone}(0, 0, \infty) = \frac{1}{2K_{sk}}\int_0^h \int_0^{\frac{BW}{2}} q_v(r, z)\,dr\,dz, \quad (12)$$

where integration is carried out over the ultrasound beam radius, *BW/2* and the thickness of the bone disk, h, and r and z are the spatial integration variables. Finally, we have the expression for the temperature at the center of the bone disk:

$$T_{bone}(0, 0, \infty) = \frac{\gamma I_{SPTA}BW}{8K_{sk}}[1 - \exp\{-2\alpha_{sk}h\}], \quad (13)$$

where the coefficient γ accounts for the portion of acoustic energy absorbed by the skull wall after reflection of the ultrasonic wave, and α_{sk} is the coefficient of absorption in a skull.

To compare our theoretical prediction of ultrasound hyperthermia with those measured experimentally *in vitro*, we estimated the contribution of the reflection of acoustic energy from the interface between either blood clot, or cranial bone, and water. The coefficients of reflection for both types of clots were estimated from the acousto-mechanical properties of human and porcine clots (Nahirnyak et al. 2006). The density of human and porcine clots is $1.076{\cdot}10^3$ kg/m^3 and $1.058{\cdot}10^3$ kg/m^3, respectively, and the speed of sound is $1.6{\cdot}10^3$ m/s for both types of clots. The intensity reflection coefficient (Kinsler et al. 1982) from the interface between human or porcine clot and water is $5.2 \cdot 10^{-3}$ and $4.0 \cdot 10^{-3}$, respectively. Therefore, the reduction of amplitude as a result of reflection from the clot surface may be ignored.

Similarly, the transmission coefficients γ for sound passing through a layer of bone were estimated as a function of frequency by using the boundary conditions presented in Kinsler et al. (1982). We have considered the layer of a bone as an isotropic medium with uniform

density with the thickness of $h = 3.8 \cdot 10^{-3}$ m and with the values for the coefficient of attenuation presented in Table 1. The values for the density of human skull, $1.7{\cdot}10^3$ kg/m^3, and for the speed of sound, $3.36{\cdot}10^3$ m/s, were taken from the literature (Duck 1990; Schwan 1969). The intensity transmission coefficients, γ, for the three ultrasound center frequencies (0.12, 1.0 and 3.5 MHz), are 0.39, 0.61 and 0.65, respectively. Thus, we included this reduction of acoustic energy in eqn (13).

For our calculations of the temperature increase in clotted blood, we assume that the density, the specific heat and the thermal conductivity of human clots were $1.08{\cdot}10^3$ kg/m^3, $3.48{\cdot}10^3$ J/(kg·K) and 0.59 W/(m·K), respectively, and were $1.06{\cdot}10^3$ kg/m^3, $3.23{\cdot}10^3$ J/(kg·K) and 0.55 W/(m·K), respectively, for porcine clots (Nahirnyak et al. 2006). Note that these physical properties were measured at 20° C. The ultrasound absorption coefficients for each frequency were assumed to be equivalent to the attenuation coefficients measured previously by Nahirnyak et al. (2006). The attenuation coefficients shown in Table 1 were utilized for the calculations of the thermal elevation in clotted blood, brain and cranial bone exposed to pulsed ultrasound. Direct measurements of both ultrasonic attenuation and absorption coefficients in soft tissues at low megahertz frequencies have demonstrated that scattering can be neglected (Parker 1983; Nassiri and Hill 1986). Thus, for our calculations, we ignored the contribution from scattering in the attenuation coefficient.

The density, specific heat and thermal conductivity values used for a cranial bone are $1.7{\cdot}10^3$ kg/m^3, $1.59{\cdot}10^3$ J/(kg·K) and 1.16 W/(m·K), respectively (Duck 1990; Lehmann and DeLateur 1982). The values for frequency-dependent absorption coefficients utilized for the numerical calculations are presented in Table 1 (ICRU report 1998; Coussios et al. 2002; Hueter 1952; Hill et al. 2004; Goldman and Hueter 1956).

A peak-to-peak pressure at the focus of ultrasound transducers of 0.25 MPa was identical for all frequencies and in all experiments. Although it seems obvious that the higher frequency brings about the higher temperature elevation as a result of higher ultrasound absorption, it is not true in our case because the temperature elevation depends also on the spatial average, temporal average intensity. At higher frequencies, the ultrasonic BW was less and, as a result, the spatial average, temporal average intensity was lesser. To proceed with the theoretical calculations of the temperature increase, the spatial average time average intensity, I_{SATA}, within the volume of a clot and across the cross section of the bone disk was computed for each frequency by using the numerical calculations of the field produced by unfocused and focused transducers (Mast and Yu 2005; Hasegawa et al. 1986). The I_{SATA} values for each frequency (0.12, 1.0 and 3.5 MHz) were estimated to be 0.39, 0.31 and 0.14 W/cm^2, respectively, for the human clots with an average diameter of 6.7 ± 0.7 mm and 0.38, 0.29 and 0.12 W/cm^2 for the porcine clots, with an average diameter of 7.8 ± 0.5 mm. The I_{SATA} values across the corresponding BW on the surface of the front face of a cranial bone disk were 0.11, 0.18 and 0.20 W/cm^2, respectively.

Table 1. Coefficients of ultrasound attenuation used in numerical calculations of temperature elevation in human skull, brain, clotted blood and porcine clotted blood (in Np/cm)

	Attenuation coefficient (Nepers/cm)			
Frequency (MHz)	Human skull	Human brain	Human clotted blood	Porcine clotted blood
0.12	0.12	0.004	0.09	0.10
1.00	1.5	0.07	0.17	0.17
3.50	7.8	0.35	0.23	0.30

The data were compiled from ICRU (1998), Hueter (1952), Hill et al. (2004), Goldman and Hueter (1956) and Nahirnyak et al. (2006).

The use of I_{SATA} in our calculations as an input parameter for intensity in eqns (8) and (13) is justified because the heating rates are low, so that heat will be conducted fairly uniformly throughout the clot or bone. Thus, the overall heating should not depend much on the detailed beam shape, but only on the average heat deposited per unit time. According to our experimental observations, the steady state temperature remains the same after the temperature reaches a maximum at the given level of intensity.

Numerical calculations and theoretical estimates were made using MATLAB (The MathWorks, Inc., Natick, MA, USA) and Mathematica (Wolfram Research, Inc., Champaign, IL, USA).

Experimental apparatus

The experimental setup for the measurement of ultrasound hyperthermia is shown in Fig. 3. Each of three transducers (unfocused 0.12 MHz, unfocused 1 MHz and focused 3.5 MHz) were driven separately by a function generator (Model 33250, Agilent Technologies, Inc., Palo Alto, CA, USA) and a radiofrequency amplifier in an acrylic tank ($41 \times 21 \times 21$ cm^3) filled with deionized water. The temperature in the water bath was kept fixed at 37.0 ± 0.1° C with a microprocessor-controlled circulator (Model EX111, Neslab Instruments, Inc., Newington, NH, USA). An inline air trap (Terumo Inc., Indianapolis, IN, USA) was used to reduce the number of bubbles entrained in the circulating water. The unfocused 0.12-MHz transducer was driven by a linear amplifier (Ultra series 2021LF/HF, T&C Power Conversion Inc.,

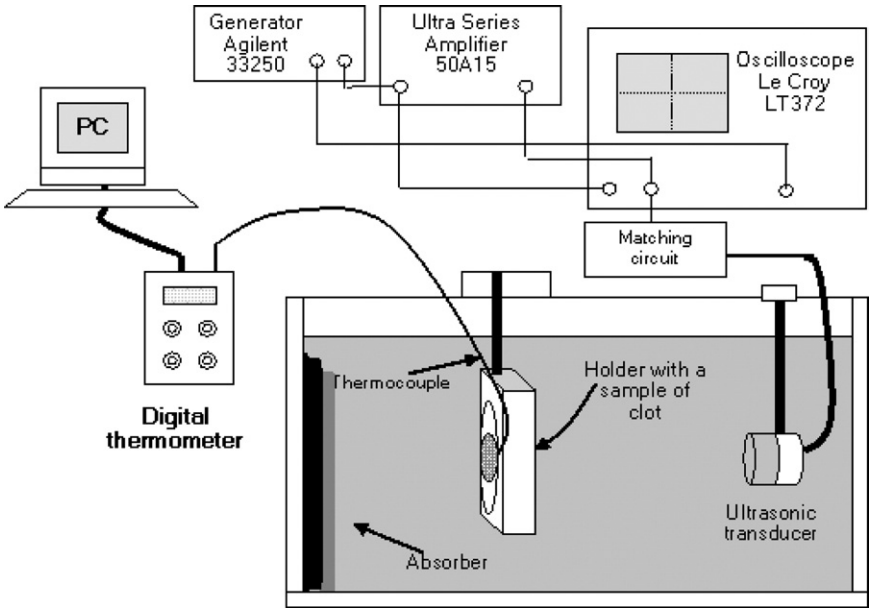

Fig. 3. Block diagram of the experimental setup for the measurements of ultrasound hyperthermia in blood clots and cranial temporal bone. Temperature in the water tank was 37° C. The sample holder was placed at the focal plane of each transducer.

Rochester, NY, USA). The unfocused 1.0-MHz and focused 3.5-MHz transducers were driven by a second amplifier (Model 150LA, Ampiflier Research, Souderton, PA, USA). The excitation signals were monitored by a 500-MHz digital oscilloscope (Model LT372, LeCroy Corp., Chestnut Ridge, NY, USA). A sheet of absorbing material was placed at a 45° angle along the far wall of the acrylic tank to minimize reflections. The resulting temperature in a clot was registered by a digital thermometer (HH 506-R, Omega Engineering, Inc., Stanford, CT, USA), connected to thermocouples either fixed to or embedded directly in the samples and recorded on a personal computer (Dell Inc., Round Rock, TX, USA).

The peak-to-peak pressure output of each ultrasound transducer and the axial and transverse beam profiles were evaluated in a preliminary calibration protocol in a water tank at room temperature (20 ± 1° C). The measured focal length and –3 dB BW for each transducer are presented in Table 2. The position of the focus or Rayleigh distance corresponds to the position of the last axial maximum of pressure. During hyperthermia experiments in clotted blood and cranial bone, the peak-to-peak pressure output was fixed at 0.25 MPa, which is equivalent to a spatial peak temporal average intensity of 0.4 W/cm^2 at the focus of ultrasound transducers and the 80% duty cycle. A duty cycle of 80% was chosen because experiments with 0.12-MHz ultrasound-assisted thrombolysis demonstrated maximum thrombolytic efficacy using this parameter (Holland et al. 2002). The pulse repetition frequency for all experiments was 100 Hz. This particular exposure level was chosen because previous studies demonstrated that both stable and inertial cavitation thresholds of clotted blood immersed in plasma were well above this value (Datta et al. 2006). Thus at an I_{SPTA} of 0.4 W/cm^2, we may exclude cavitation as a factor contributing to the enhanced thrombolysis.

Sample preparation

Whole blood clots were prepared by aliquoting 1.5 mL arterial porcine or venous human blood into the 8-mm inner diameter glass Vacutainer tubes (Franklin Lakes, NJ, USA), immersing the tubes in a 37° C water bath for three hours and storing the clots at 5° C before use in comparative ultrasound and rt-PA studies, which ensured complete clot retraction. Human whole blood was drawn from 10 healthy volunteers by sterile venipuncture after local institutional review board approval. Additional aliquots of blood from each pig or human were used to obtain a complete coagulation panel from Antech Diagnostics (Chicago, IL, USA), including D-dimer, activated partial thromboplastin time (aPTT), fi-

Table 2. Spatial characteristics of transducers used in the measurements of ultrasound-induced heating

Transducer frequency (MHz)	Transducer aperture (mm)	−3 dB beam width (mm)	Focal length (mm)
0.12	61.4	22.0	74
1.00	25.0	7.0	94
3.50	19.0	2.5	93

Calibration of transducers was performed at 20°C.

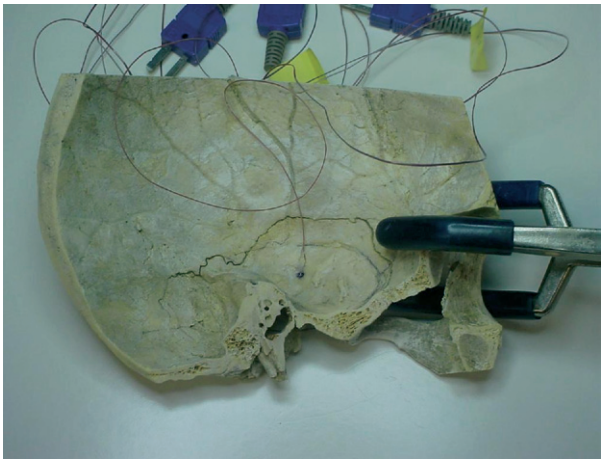

Fig. 4. A segment of dry human skull with the thermocouple attached to the center of the distal surface of a temporal bone.

brinogen and prothrombin time testing, as well as a complete blood count. Most pigs used as part of this study were found to be slightly anemic, with hematocrits in the range of 25% to 35%. Only donors with values in the range 10 to 900 ng/mL for the D-dimer test, 10 to 25 *s* for aPTT, 250 to 700 mg/dL for the fibrinogen concentration and 9 to 13 s for prothrombin time were considered to be acceptable. The resulting clots shown in Fig. 2 were normally dark red in color and roughly cylindrical in shape, with an average diameter of 7 to 10 mm, and a mass of 0.5 g.

Human fresh-frozen plasma (hFFP) was procured from a blood bank in 250- to 300-mL units. Each unit was briefly thawed, aliquoted into 50-mL centrifuge tubes (Fisher Scientific Research, Pittsburgh, PA, USA) and stored at –70° C. Aliquots of plasma were allowed to thaw for experiments, and the remaining amounts discarded after completion of a given experiment.

An acrylic sample holder with a round acoustically transparent window 70 mm in diameter was used to position the clot samples at the location of the focus of each transducer. The windows were comprised of Tegaderm (3M Health Care, St. Paul, MN, USA) and the sample holder was filled with plasma surrounding the blood clot. Porcine plasma was used for the porcine clots and human plasma was used for human clots. The sample holder had two ports within the side walls: one for fixation of the thermocouple and the other to allow entrapped air to be removed from the sample during the degassing process. The sample holder was placed in a vacuum chamber connected to a pump (Model 8803, Welch Vacuum Technology. Inc., Skokie, IL, USA), which lowered the pressure to that of the vapor pressure of plasma for approximately 85 min. The pressure was allowed to return to atmospheric pressure gently, the bleed valve was closed and the holder was placed in the focal region of the transducer in the water tank.

Temperature measurement techniques

The ratio of the thermocouple diameter to the acoustic wavelength was less than 1/25 for all three frequencies. Under such conditions, we eliminated an artifactual temperature rise in our measurements because of viscous heating and absorption in the thermocouple itself (Hynynen and Edwards 1989; Goss et al. 1977). The duration of each ultrasound-induced hyperthermia measurement was 5 min. For the experiments using 120-kHz pulsed ultrasound exposure, a hypodermic *T*-type thermocouple (HYP0–33, Omega Engineering, Stamford, CT, USA) with a tip diameter 203 μm was employed. For hyperthermia measurements at 1 MHz, we used a bare wire *E*-type thermocouple (CHCO-001, Omega Engineering, Inc., Stamford, CT, USA) with a diameter of 25 μm. A bare-wire *E*-type thermocouple (CHCO-0005, Omega Engineering, Inc.) with a diameter of 12 μm was used for the temperature measurements at 3.5 MHz. Each thermocouple tip was positioned approximately in the center of the clot sample by marking the clot radius on the thermocouple and inserting the thermocouple into the clot up to the mark. The block diagram of the experimental apparatus is shown in Fig. 3.

A 15-cm, 111.6-g segment of a human skull immersed in deionized water, shown in Fig. 4, was degassed in the vacuum chamber described previously for 85 min. The thickness of the skull at the level of the temporal bone was estimated to be 3.8 ± 0.1 mm. Two bare-wire *E*-type thermocouples (5TC-TT Omega En-

Table 3. Numerical estimates for the temperature rise in human cranial bone, porcine and human clotted blood and human brain tissue exposed to pulsed ultrasound (I_{SPTA} = 0.4 W/cm^2) for 300 s at three frequencies

Frequency (MHz)	T (°C) in temporal bone	T (°C) in porcine clot	T (°C) in human clot	T (°C) in human brain tissue
0.12	0.32	0.58 (+0.20, −0.13)	0.38 (+0.32, −0.16)	0.02
1.00	1.25	0.71 (+0.22, −0.15)	0.55 (+0.37, −0.19)	0.24
3.50	0.71	0.49 (+0.48, −0.26)	0.33 (+0.25, −0.13)	0.44

An estimate of the propagated errors for the theoretical prediction of temperature elevation in clotted blood appears in parentheses.

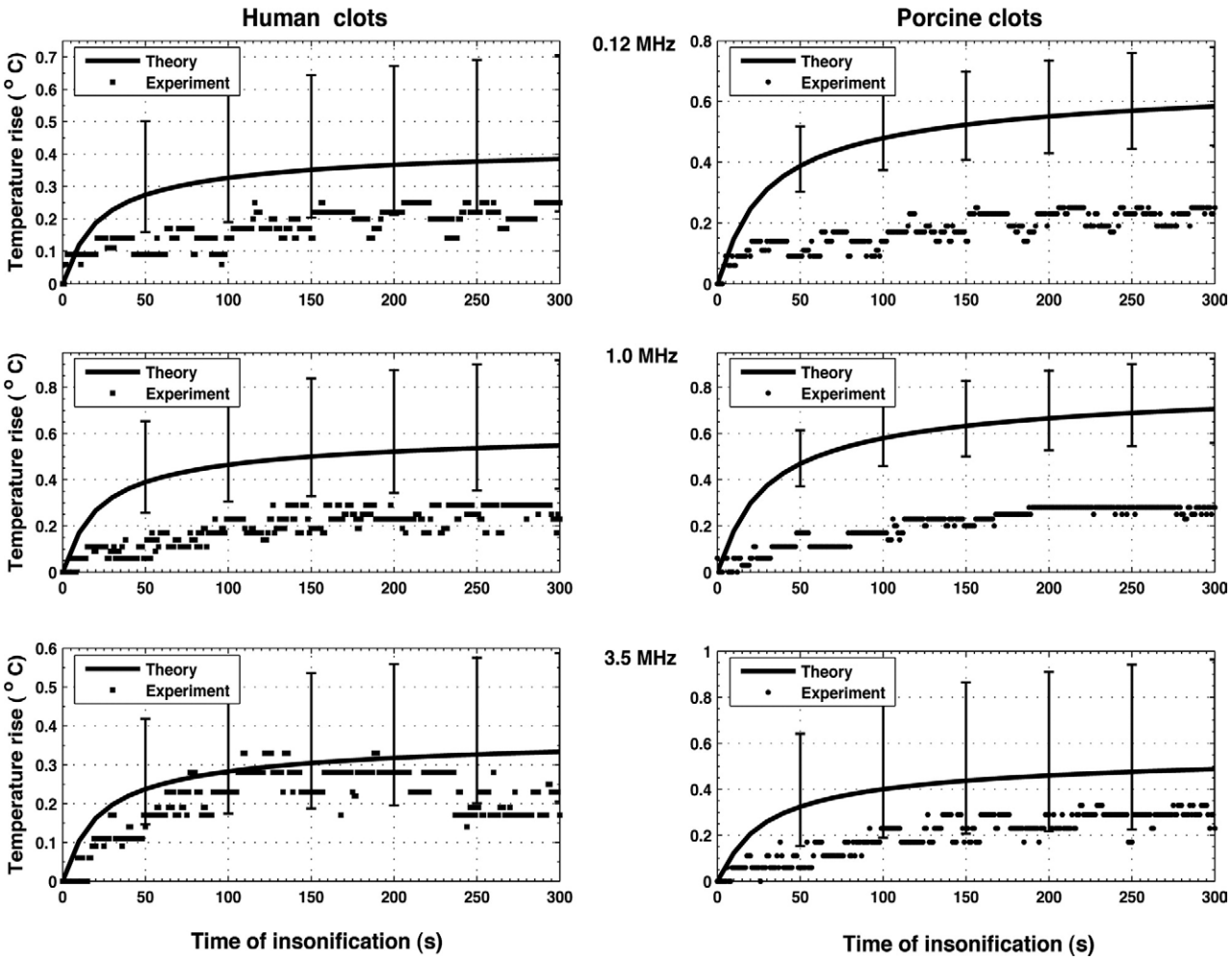

Fig. 5. Results of the theoretical calculations (solid) and averaged experimental data (dots) of ultrasound hyperthermia in human (left) and porcine (right) clotted blood at three frequencies: 120 kHz, 1.0 MHz and 3.5 MHz. Error bars represent the propagated error in the theoretical calculations.

gineering, Inc.) with a diameter of 127 μm were glued to the temporal bone with cyanoacrylate glue. One of the thermocouples was fixed on the proximal surface of the bone and the other was fixed to the distal surface. The thermocouples were positioned in the focal region of each transducer. The precision of all thermocouple measurements was 0.06° C.

RESULTS

Using eqns (8) and (13), the predicted values for ultrasound-induced heating in porcine or human clots and bone in the frequency range between 0.12 and 3.5 MHz are presented in Table 3. The temporal dependence of the temperature increase in blood clots exposed to pulsed ultrasound with an I_{SPTA} of 0.4 W/cm^2 is shown in Fig. 5. The solid lines represent theoretical prediction of the temperature increase and the data points represent experimentally measured thermal elevation. Experimental data points represent the average values for the temperature rise obtained in two *in-vitro* experiments. The error bars in the theoretical curves were assessed by combining the effects of the range of acousto-mechanical and thermal properties measured in the clotted blood, as well as the size range of the heat source, which depends on the physical dimensions of the clots.

Note that the theoretical estimates for the thermal increase in clots as a result of ultrasound exposure to 0.4 W/cm^2 pulsed ultrasound (I_{SPTA} = 0.4 W/cm^2) do not exceed 0.88° C for any of the three frequencies. Both the theoretical and experimental data show an initial temperature increase followed by a steady state temperature regime. Implicit in the derivation of the predicted thermal increase is a calculation of the reflected and absorbed ultrasonic energy. Also included in the calcula-

Table 4. Experimental results for the maximum temperature rise measured in tissue exposed to pulsed ultrasound (PRP=10 *ms*, $P_{p\text{-}t\text{-}p}$ = 0.25 MPa, I_{SPTA}= 0.4 W/cm^2, T = 37 °C, *t* = 300 *s*) *in vitro*

Frequency (MHz)	T (°C) on surface of temporal bone		T (°C) in center of porcine clot	T (°C) in center of human clot
	Proximal	Distal		
0.12	0.61	0.45	0.25	0.25
1.00	1.00	0.90	0.28	0.29
3.50	0.85	0.29	0.33	0.33

tion is the beam aperture, which was not identical for the three frequencies. The 3.5-MHz transducer was focused and the beam diameter is smaller than that of the 0.12 and 1.0 MHz unfocused beams. Thus the predicted temperature increase at 3.5 MHz in clotted blood is less than the temperature increase calculated at either 0.12 or 1.0 MHz.

To estimate the maximum temperature rise expected in human clotted blood and brain, eqn (8), which uses a heated sphere model, was used to calculate the temperature elevation values at the center of a sphere of 6.7 mm in diameter. Similarly, eqn (13), which uses a heated disk model, was used to predict the maximum temperature increase in cranial bone as a function of incident intensity. The results of the numerical calculations for the 0.12-, 1.0- and 3.5-MHz transducers characterized in Table 2 are presented in Table 3. These temperatures demonstrate that, at 120 kHz, we have the maximum temperature rise in clotted blood rather than in cranial bone or brain tissue. Measured values of the maximum temperature increase in porcine and human blood clots and in human temporal bone exposed to pulsed ultrasound (I_{SPTA} = 0.4 W/cm^2) are presented in Table 4. The maximum temperature increase in clotted blood (0.33 ± 0.04° C for both types of clots) was noted at 3.5 MHz. The temperature rise in cranial bone exposed to a pulsed ultrasound was greater than the temperature increase in blood clots at each frequency. Note that any of the three frequencies, the temperature increase on the surface of human cranial bone does not exceed 1° C. The maximum thermal elevation of 1.00 ± 0.06° C was achieved on the proximal surface of the cranial bone exposed to 1-MHz pulsed ultrasound. No appreciable difference in the temperature elevations between the proximal and distal surfaces of the bone were observed for 0.12 and 1 MHz. However, at 3.5 MHz, the temperature elevation on the proximal wall is somewhat higher (0.4–0.6° C). The temperature on the proximal and distal bone surfaces is plotted for one measurement run as a function of time in Fig. 6. For all ultrasound heating measurements in both bone and clotted blood, a steady-state temperature increase was achieved after an initial 30- to 120-s period of insonification.

DISCUSSION

The theoretical prediction of the temperature elevation at the center of human and porcine clots presented in Fig. 5 tends to overestimate the actual temperatures measured, sometimes by a factor of two. Several factors could contribute to this discrepancy, including errors in the assumed size and shape of the clot, the absorption coefficient used or the position of the thermocouple within the clot. According to eqns (8) and (10), the temperature increase is linearly proportional to the square of the radius of a clot, so any error in the measurement of the clot size is squared. Note that scattering was ignored and the coefficient of absorption was assumed to be identical to the coefficient of attenuation. Note also that the absorption coefficient for human and porcine clots was measured at 20° C, but our experiments were conducted at 37° C. Note that these combined errors contribute to the error bars shown in Fig. 5. In addition, the positioning of the thermocouple tip inside the clot samples could have been off center and we did not monitor the thermocouple placement during the experiments. Because the temperature is expected to decrease with distance from the center of a clot, the thermocouple location might contribute to the measurements of the temperature increase appearing lower than the theoretical predictions. At 3.5 MHz, the experimental data falls within the error bounds in the theory. Our theoretical model and our experimental set-up did not incorporate blood perfusion. Thus, actual *in-vivo* temperature increases will likely be lower.

As shown in Fig. 5, the theoretical prediction of the initial heating rate of human clots exposed to 3.5-MHz

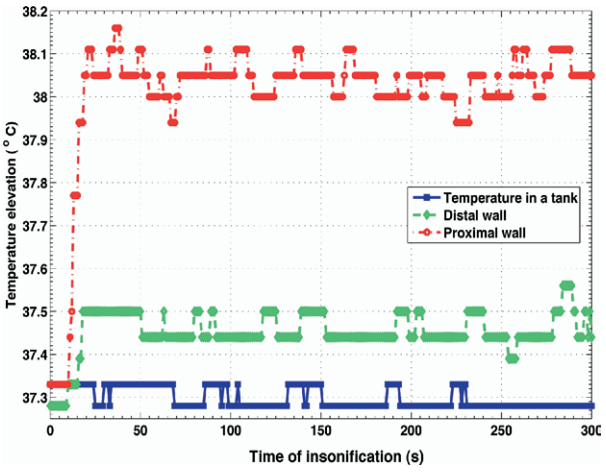

Fig. 6. An example of the temperature development on both faces of the human temporal cranial bone during insonification at 3.5 MHz with an 80% duty cycle at 37° C. The spatial peak, temporal average intensity was 0.4 W/ cm^2. The diameter of the ultrasonic beam was 2.5 mm.

pulsed ultrasound (I_{SPTA} = 0.4 W/cm^2) was 0.01° C/s. The slope in the initial heating regime corresponds to an adiabatic heating rate, where heat conduction is ignored. A rough estimate of the heating rate in soft tissue exposed to pulsed ultrasound was presented by Nyborg and Ziskin (1985) and is given by a simple empirical formula that depends on the attenuation coefficient and the spatial average, temporal average intensity. Using the attenuation coefficient for clotted blood and a spatial average, temporal average intensity of 0.4 W/cm^2, their formula yields an estimate of the heating rate of 0.01° C/s, which is consistent with our data.

Our theoretical results may also be compared with previous *in-vivo* experiments on low-intensity ultrasound exposure of soft tissues. In one study, temperature rise was quantified in human muscle exposed to 3.0-MHz pulsed ultrasound with a spatial average, temporal average intensity of 0.5 W/cm^2 for 10 min (Gallo et al. 2004). A temperature increase of 2.8° C was noted in these *in-vivo* experiments. Using eqn (10) and using the exposure parameters of Gallo et al. (2004) and the absorption coefficient of 0.26 Np/cm for human skeletal muscle, the predicted temperature increase is 2.5° C, which is consistent with their measured value of 2.8° C. Similarly, Carstensen et al. (1990) measured the temperature elevation in rat liver exposed to 2.0-MHz continuous wave ultrasound with an I_{SATA} of 0.57 W/cm^2. The maximum temperature increase measured by these investigators in rat liver was 1.8° C. Using the same ultrasound exposure parameters as input to eqn (10) in human liver with an absorption coefficient of 0.132 Np/cm (ICRU 1998), a 1.3° C temperature increase is predicted, which is also consistent with their experimental data.

The temperature elevations measured in blood clots exposed to low-intensity (<0.5 W/cm^2) pulsed ultrasound were extremely small (~0.2° C) for all three frequencies (0.12, 1.0 and 3.5 MHz) shown in Fig. 5. In addition, for the attenuation values assumed here, the thermal elevation in clotted blood, shown in Fig. 5, will be higher than in brain tissue for frequencies less then 1 MHz as it follows from Table 3. Enhanced rt-PA thrombolysis has been demonstrated *in vitro* in both human and porcine clots exposed to low-intensity ultrasound (Holland et al. 2002) with the same conditions explored here at 0.12 and 1.0 MHz. Therefore, it is unlikely that a thermal mechanism will contribute significantly to thrombolytic enhancement for frequencies less than 3.5 MHz with intensities less than 0.5 W/cm^2.

CONCLUSIONS

The temperature rise in human cranial bone and porcine and human blood clots was determined experimentally at 37° C *in vitro* in the frequency range between 120 kHz and 3.5 MHz. Ultrasound insonification of human temporal cranial bone with a spatial peak temporal average intensity of 0.4 W/cm^2 at 1 MHz produces a maximum temperature rise of 1.0° C on the proximal side of the skull bone. There was no substantial thermal elevation at the center of blood clots immersed in plasma and insonified with the same level of ultrasound intensity in this frequency range. The theoretical estimates of the magnitude of thermal elevation during ultrasonic insonification of the blood clots and cranial bone are higher than those measured experimentally. Thus temperature increases predicted by the theory may overestimate the actual temperature rise. In the presence of perfusion, the mild thermal elevation within the volume of a clot, on its surface and on the surface of the cranial bone, would be even smaller.

Understanding the potential for ultrasound heating of blood clots during ultrasound-assisted thrombolysis is an important first step in improving thrombolytic efficacy while minimizing unwanted thermal bioeffects. These theoretical results can also be used to predict the temperature elevation in tissue as a function of spatial average, temporal average intensity. The prediction of temperature elevations in cranial bone and blood clots exposed to pulsed ultrasound may be helpful in the development of high-intensity focused ultrasound and other therapeutic ultrasound applications.

Acknowledgments—This research was supported by the National Institutes of Health (grant number NIH/NINDS R01-NS047603). The authors gratefully thank Dr. Jason Meunier, Sampada Vaidya, Jun Tan, Ashima Dhamija and Nazli Bavani for the help in preparation of the blood clot samples. We also thank Drs. George Shaw and Louis McAdory for very helpful discussions of the data and Kate Williams for help in conducting the ultrasound heating experiments and processing the results.

REFERENCES

Alexandrov AV, Molina CA, Grotta JC, Garami Z, Ford SR, Alvarez-Sabin J, Montaner J, Saqqur M, Demchuk AM, Moye LA, Hill MD, Wojner AW. Ultrasound-enhanced systemic thrombolysis for acute ischemic stroke. N Engl J Med 2004;351(21):2170–2178.

Atar S, Rosenschein U. Perspectives on the role of ultrasonic devices in thrombolysis. J Thromb Thrombolysis 2004;17(2):107–114.

Atar S, Luo H, Birnbaum Y, Hansmann D, Siegel RJ. The use of transducer-tipped ultrasound catheter for recanalization of thrombotic arterial occlusions. Echocardiography 2001;18(3):233–237.

Atar S, Luo H, Nagai T, Sahm RA, Fishbein MC, Siegel RJ. Arterial thrombus dissolution in vivo using a transducer-tipped, high-frequency ultrasound catheter and local low-dose urokinase delivery. J Endovascular Therapy 2001;8(3):282–290.

Bekeredjian R, Chen S, Frenkel PA, Grayburn PA, Shohet RV. Ultrasound-targeted microbubble destruction can repeatedly direct highly specific plasmid expression to the heart. Circulation 2003;108(8):1022–1026.

Schwan HP, ed. Biological Engineering. New York: McGraw-Hill, 1969:214–222.

Blinc A, Francis CW, Trudnowski JL, Carstensen EL. Characterization of ultrasound-potentiated fibrinolysis in vitro. Blood 1993;81(10):2636–2643.

Carstensen EL, Child SZ, Norton S, Nyborg W. Ultrasound heating of the skull. J Acoust Soc Am 1990;87(3):1310–1317.

Cheng R. Physical Chemistry. New York: Random House, 1981.

Coussios C-C, Holland CK, Shaw GJ. Transmission of a large unfocused 120-kHz and 1-MHz ultrasound beam through the human skull. J Acoust Soc Am 2002;112:2433.

Datta S, Coussios C-C, McAdory LE, Tan J, Porter T, De Courten-Myer G, Holland CK. Correlation of cavitation with ultrasound enhancement of thrombolysis. Ultrasound Med Biol 2006;32(8): 1257–1267.

Duck FA. Physical properties of tissue: A comprehensive reference book. London: Academic Press, 1990.

Duckett AS, Reid AD, Leamen L, Cucevic V, Foster FS. Thermal assessment of 40-MHz ultrasound at soft tissue-bone interfaces. Ultrasound Med Biol 2004;30(5):665–673.

Everbach EC, Francis CW. Cavitational mechanisms in ultrasound-accelerated thrombolysis at 1 MHz. Ultrasound Med Biol 2000; 26(7):1153–1160.

Francis CW, Onundarson PT, Carstensen EL, Blinc A, Meltzer RS, Schwarz K, Marder V. Enhancement of fibrinolysis in vitro by ultrasound. J Clin Invest 1992;90:2063–2068.

Francis CW, Blinc A, Lee S, Cox C. Ultrasound accelerates transport of recombinant tissue plasminogen activator into clots. Ultrasound Med Biol 1995;21(3):419–424.

Gallo JA, Draper DO, Brody LT, Fellingham GW. A comparison of human muscle temperature increases during 3-MHz continuous and pulsed ultrasound with equivalent temporal average intensities. J Orthoped Sports Phys Ther 2004;34(7):395–401.

Goldman DE, Hueter TF. Tabular data of the velocity and absorption of high-frequency sound in mammalian tissues. J Acoust Soc Am 1956;28(1):35–37.

Harpaz D, Chen X, Francis CW, Marder VJ, Meltzer RS. Ultrasound enhancement of thrombolysis and reperfusion in vitro. J Am Coll Cardiol 1993;21:1507–1511.

Hasegawa T, Matsuzawa K, Inoue N. A new expansion for the velocity potential of a circular concave piston. J Acoust Soc Am 1986;79(4): 927–931.

Hill CR, Bamber JC, ter Haar J GR. Physical principles of medical ultrasonics. Chichester, England: Wiley & Sons, Ltd. 2004:123.

Holland CK, Vaidya SS, Coussios C-C, Shaw GJ. Thrombolytic effects of 120 MHz and 1 MHz ultrasound and tissue plasminogen activator on porcine whole blood clots. J Acoust Soc Am 2002;112: 2370.

Hueter TF. Messung der Ultrashallabsorption in menschlichen Schädelknochen und ihre Abhängigkeit von der Frequentz. Naturwissenschaften 1952;39:21–22.

Hynynen K, Edwards DK. Temperature measurements during ultrasound hyperthermia. Med Phys 1989;16(4):618–626.

International Commission on Radiation Units, Measurements. Tissue Substitutes, Phantoms, computational Modeling in Medical Ultrasound. Bethesda, MD. ICRU Report, December 31 1998;61:45–51.

Kinsler LE, Frey AR, Coppens AB, Sanders JV. Fundamentals of acoustics. New York: John Wiley, 1982.

Kudo S. Thrombolysis with ultrasound effect. Tokyo Jikeikai Med J 1989;104:1005.

Lauer CG, Burge R, Tang DB, Bass BG, Gomez ER, Alving BM. Effect of ultrasound on tissue-type plasminogen activator-induced thrombolysis. Circulation 1992;86:1257–1264.

Lehmann JF, DeLateur BJ. Therapeutic heat and cold. Baltimore: Williams & Wilkins, 1982.

Mast TD, Yu F. Simplified expansions for radiation from a baffled circular piston. J Acoust Soc Am 2005;118(6):3457–3464.

McDannold N, King RL, Hynynen K. MRI monitoring of heating produced by ultrasound absorption in the skull: in vivo study in pigs. Magn Res Med 2004;51(5):1061–1065.

Nahirnyak VM, Yoon SW, Holland CK. Acousto-mechanical and thermal properties of clotted blood. J Acoust Soc Am 2005;117: 2413.

Nahirnyak VM, Yoon SW, Holland CK. Acousto-mechanical and thermal properties of clotted blood. J Acoust Soc Am 2006;119(6): 3766–3772.

Nassiri DK, Hill CR. The use of angular acoustic scattering measurements to estimate structural parameters of human and animal tissues. J Acoust Soc Am 1986;79(6):2048–2054.

National Council on Radiation Protection, Measurements. Exposure criteria for medical diagnostic ultrasound: I. Criteria based on thermal mechanisms. Bethesda, MD. NCRP Publications, June 1 1992;113:35.

Nyborg WL. Physical mechanisms for biological effects of ultrasound. In: Surles EB, ed. Rockville, MD: The Catholic University of America and U.S. Department of Health, Education, and Welfare, Public Health Service, Food and Drug Administration, Bureau of Radiological Health 1978:3.

Nyborg WL. Solutions of the bio-heat transfer equation. Phys Med Biol 1988;33:785–792.

Nyborg WL, Ziskin MC. Biological effects of ultrasound. New York: Churchill Livingstone, 1985.

Nyborg WL, Wu J. Solution of the linear bioheat transfer equation. Phys Med Biol 1994;39:924–925.

Parker KJ. Ultrasonic attenuation and absorption in liver tissue. Ultrasound Med Biol 1983;9(4):363–369.

Pfaffenberger S, Devcic-Kuhar B, Kastl SP, Huber K, Maurer G, Wojta J, Gottsauner-Wolf M. Ultrasound thrombolysis. Thromb Haemost 2005;94(1):26–36.

Morse PM, Feshbach H. Methods of theoretical physics. New York: McGraw-Hill, 1953;857–861.

Rosenschein U, Roth A, Rassin T, Basan S, Laniado S, Miller HI. Analysis of coronary ultrasound thrombolysis endpoints in acute myocardial infarction (ACUTE trial). Results of the feasibility phase. Circulation 1997;95(6):1411–1416.

Sakharov DV, Hekkenberg RT, Rijken DC. Acceleration of fibrinolysis by high-frequency ultrasound: The contribution of acoustic streaming and temperature rise. Thromb Res 2000;100(4):333–340.

Shaw GJ, Hahn NL, Wagner KR, Kanter DS, Holland CK. Ultrasound assisted clot lysis for stroke therapy. J Acoust Soc Am 2001a;109: 2456.

Shaw GJ, Hahn NL, Wagner KR, Kanter DS, Holland CK. Ultrasound assisted thrombolysis in an in vitro clot model. Acad Emerg Med 2001b;8.

Shaw GJ, Dhamija A, Holland CK, Wagner KR. Temperature dependence of tPA thrombolysis in an in vitro clot model. Acad Emerg Med 2003;10:438–439.

Shaw GJ, Bavani N, Dhamija A, Lindsell CJ. Effect of mild hypothermia on the thrombolytic efficacy of 120 kHz enhanced thrombolysis in an in-vitro human clot model. Thromb Res 2006;117:603–608.

Suchkova V, Carstensen EL, Francis CW. Ultrasound enhancement of fibrinolysis at frequencies of 27 to 100 kHz. Ultrasound Med Biol 2002;28(3):377–382.

Olsson SB, Johansson B, Nilsson AM, Olsson C, Roijer A. Enhancement of thrombolysis by ultrasound. Ultrasound Med Biol 1994; 20:375–382.

Taniyama Y, Tachibana K, Hiraoka K, Namba T, Yamasaki K, Hashiya N, Aoki M, Ogihara T, Yasufumi K, Morishita R. Local delivery of plasmid DNA into rat carotid artery using ultrasound. Circulation 2002;105(10):1233–1239.

Vella GJ, Humphrey VF, Duck FA, Barnett SB. Ultrasound-induced heating in a foetal skull bone phantom and its dependence on beam width and perfusion. Ultrasound Med Biol 2003;29(6):779–788.

Wolpert SM, Bruckmann H, Greenlee R, Wechsler L, Pessin MS, del Zoppo GJ. Neuroradiologic evaluation of patients with acute stroke treated with recombinant tissue plasminogen activator. AJNR Am J Neuroradiol 1993;14(1):3–13.